Scientific Paper / Artículo Científico

UNIVERSIDAD POLITÉCNICA SALESIANA ECUADOR
INGENIUS
Revista de Ciencia y Tecnología
https://doi.org/10.17163/ings.n29.2023.04
pISSN: 1390-650X / eISSN: 1390-860X

Study of the Energy Efficiency of an Urban E-Bike Charged with a Standalone Photovoltaic Solar Charging Station and its Compliance with the Ecuadorian Grid Code No. Arcernnr – 002/20

Estudio de Eficiencia Energética de una Bicicleta Eléctrica Urbana Cargada con una Estación de Carga Solar Fotovoltáica Autónoma y su Cumplimiento con la Regulación Ecuatoriana No. Arcernnr – 002/20

Vinicio Iñiguez-Morán[1,*], Edisson Villa-Ávila[1],
Danny Ochoa-Correa[2], Ciro Larco-Barros[2], Rodrigo Sempertegui-Álvarez[1]

Received: 02-08-2022, Received after review: 20-10-2022, Accepted: 10-11-2022, Published: 01-01-2023

Abstract

E-bikes are an emerging sustainable means of transportation, if adopted massively, they can help face the challenges of human mobility in urban centers worldwide. In Cuenca, Ecuador, the local government built cycle routes (13.47 km) connecting strategic points to facilitate and encourage sustainable mobility. However, the effective implementation of the electromobility strategies at a large scale entails impacts on the power grid, like the increase in the energy demand and the possible decrease of the energy quality due to the harmonic distortion that characterizes the battery's charging current. This research aims to obtain a primary input to evaluate such impacts through an energy efficiency study of an urban e-bike charged by a standalone solar photovoltaic charging station implemented in the Microgrid Laboratory of Universidad de Cuenca.

Resumen

Las bicicletas eléctricas (*e-bikes*) son un medio de transporte sostenible emergente. Si se adoptan masivamente, ayudarían a enfrentar los desafíos de movilidad humana en las ciudades del mundo. En Cuenca, Ecuador, el gobierno local construyó ciclovías (13,47 km) que conectan puntos estratégicos, para facilitar y fomentar la movilidad sostenible. Sin embargo, la implementación efectiva de las estrategias de electromovilidad a gran escala conlleva impactos en la red eléctrica, como el aumento de la demanda de energía y la posible disminución de su calidad debido a la distorsión armónica de la corriente de carga de la batería. El propósito de esta investigación es hacer una evaluación preliminar de dichos impactos, mediante el estudio de eficiencia energética de una *e-bike* urbana cargada con una estación solar fotovoltaica aislada, implementada en el Laboratorio de Micro-Red de la Universidad de Cuenca.

[1,*] Laboratorio de Micro-Red, Universidad de Cuenca, Ecuador.
Corresponding author ✉: vinicio.iniguezm@ucuenca.edu.ec
[2]Facultad de Ingeniería, Universidad de Cuenca, Ecuador.

Suggested citation: Íñiguez-Morán, V.; Villa-Ávila, E.; Ochoa-Correa, D.; Larco-Barros, C. and Sempértegui-Álvarez, R. "Study of the Energy Efficiency of an Urban E-Bike Charged with a Standalone Photovoltaic Solar Charging Station and its Compliance with the Ecuadorian Grid Code No. Arcernnr – 002/20". *Ingenius, Revista de Ciencia y Tecnología*. N.° 29, (january-june). pp. 46-57. 2023. DOI: https://doi.org/10.17163/ings.n29.2023.04.

The methodology includes the experimental characterization of the battery's charging regime, the vehicle's energy efficiency calculation, and the evaluation of its compliance with Ecuadorian grid code No. ARCERNNR – 002/20. Results show that the battery's charger performs a charging regime standardized by German regulations, delivering 92% of charge in 4.82 hours. The e-bike's calculated average energy efficiency is 2.18 kWh/100 miles or 73.77 m/Wh, and a fuel economy of 1545.1 MPGe. Finally, the magnitude of the first four odd harmonic components and the total harmonic distortion of the charging current exceeds the limits established by the grid code in force.

Keywords: e-Bike, Electromobility, Power Quality, Lithium-Ion Batteries, Grid code No. ARCERNNR 002/20, Std. DIN 41772

La metodología incluye la caracterización experimental del régimen de carga de la batería, el cálculo de la eficiencia energética del vehículo y la evaluación del cumplimiento de la normativa ecuatoriana No. ARCERNNR–002/20. Los resultados muestran que el cargador de la batería implementa un régimen de carga estandarizado por normas alemanas, entregando 92% de carga en 4,82 horas. La eficiencia energética promedio de la *e-bike* es 2,18 kWh/100 millas o 73,77 m/Wh, y una economía de combustible de 1545,1 MPGe. Finalmente, la magnitud de las primeras cuatro componentes armónicas impares y la distorsión armónica total de la corriente de carga supera los límites establecidos por la normativa.

Palabras clave: bicicleta eléctrica, electromovilidad, calidad de energía, batería de iones de litio, resolución N.° ARCERNNR 002/20, Est. DIN 41772

1. Introduction

Nowadays, many urban population centers worldwide are experiencing serious problems related to vehicular congestion, negatively impacting people's quality of life. Its main manifestation is the progressive reduction in traffic speeds, observed in increases in travel times, consumption of fossil fuels, other operating costs, and atmospheric pollution, concerning a traffic flow free of traffic jams [1].

Therefore, the authorities, the different social actors and citizens have used some strategies aimed at mitigating these impacts. These strategies follow various paths, such as improving the mass public transport offer (in terms of fares and routes), restricting the access of private transport in urban centers, promoting fleets of energy-efficient vehicles, and promoting modes of transportation of low environmental impact [2]. Among the initiatives that are part of this last strategy, micromobility has been gaining relevance as an increasingly widespread transport solution [3].

Micromobility refers to using a wide variety of private or shared light vehicles that operate at low speeds and for short trips; it includes electric bicycles (e-bikes), electric scooters (e-scooters) and electric mopeds. The way people travel in urban areas is rapidly changing as this concept is quickly adopted and promoted to achieve a more sustainable transportation system [4]. The growing popularity of electric micromobility means has gained the interest of scientists around the world, a fact reflected in a considerable number of research works. In the literature, many papers address legislative issues related to micromobility, perhaps motivated mainly by the report "Global EV Outlook 2020 - Entering the decade of electric drive?" published by the International Energy Agency (IEA) in 2020 [5].

For example, the authors in [6] showed that European Union (EU) countries and the United Kingdom (UK) have different approaches to electromobility means in legal terms, considering them as a means of micro transportation or personal transport. In addition, this work shows that in some countries, electromobility means such as e-scooters are not defined in regulations, but other rules apply (e.g., regulations for bicycles). The fact that such regulations consider users of micromobility means as pedestrians or cyclists massifies them in urban environments, generating the need to develop detailed legislation to condition the safe movement of its users and manage them properly in cities to avoid chaos, as mentioned by researchers in [7].

In this sense, [8] presents a comparative study conducted in thirty European cities aimed at assessing the management problems of e-scooters in urban spaces. The results show that the shared use of micromobility means is becoming more and more attractive, forcing public electric energy service providers to assume significant increases in the loadability of their networks.

In the United States of America (USA) context, researchers in [9] show that people often prefer electric micromobility modes to cars, especially in many USA cities. Moreover, in the same work, the authors claim that electric micromobility modes could complement public transport, emphasizing the modal integration and social benefits of introducing a shared-use model. On the other hand, researchers in [10] studied the impact of time variables, such as weather data and time-invariant variables on the expected demand for micromobility means (taking e-scooters as a case) in Chicago (USA). The authors focused on determining the location of e-scooter charging stations and found that economic factors were decisive in this task. Similarly, authors in [11] considered a multi-objective stochastic location assignment model for e-scooter battery swapping stations. In [12], the study focused on finding an optimization model to define the location of multiple charging stations of different technical characteristics for electric micromobility vehicles.

Then, in the Latin American context, interesting works in [13, 14] report electromobility experiences in countries such as Brazil and Uruguay, respectively, while in [15], the Inter-American Development Bank (IDB) presents a more general Latin American perspective on this matter.

In the Ecuadorian context, since 2020, the most populated cities have experienced a significant increase in the demand and use of electric vehicles to meet their mobility needs [16]. According to [17, 18], the COVID-19 pandemic boosted this growth in electromobility, which affected conventional urban transport (buses and taxis) both in terms of availability and increased risk of contagion in these mass media of human mobility. A reality perceived on a global scale as well.

Although government authorities substantially eased the health restrictions established during the pandemic and reactivated public and private transport services, statistics show that the preference for using electric bicycles and scooters has remained in the main cities. This fact points to an imminent paradigm shift in mobility that neither local governments, companies, nor businesses specialized in mobility have ignored. In the city of Cuenca, the third most populated in Ecuador, the Decentralized Autonomous Government (GAD-Cuenca) has undertaken actions to facilitate and encourage sustainable mobility through a Mobility Plan [19], three of which are worth mentioning. The construction of 13.47 km of cycle routes connecting the most strategic points of the city [20]; the operation of "Tranvía de Cuenca", the mass electric transport service with 21.4 km of tracks [21]; and the implementation of charging stations in one of the city's emblematic parks [22].

Universidad de Cuenca, a public institution of higher education based in the city, launched its institutional program named MoverU, whose purpose

is to develop a sustainable mobility system based on scientific evidence that contributes to proposals and actions to solve urban transportation problems, aiming to improve people's quality of life. Within the program's initiatives, it is possible to identify micromobility projects build around using light means of transport with electric assistance. In addition, the Centro Científico Tecnológico y de Investigación Balzay (CCTI-B) of Universidad de Cuenca has the electrical Micro-grid Laboratory that constitutes a test bench for carrying out studies on using and managing renewable energy sources to meet human energy necessities cleanly and sustainably. This laboratory has different electrical generation systems: solar photovoltaic, wind, hydraulic, fuel cells, etcetera; energy storage systems: electrochemical batteries, vanadium flow batteries, hydrogen production by electrolysis, among others; and different final uses of the energy produced/stored: the electrical installations of the building that houses the laboratory, programmable electrical loads (for the emulation of consumption profiles), and electric vehicle charging stations [23].

All the characteristics listed previously make the CCTI-B's electrical Micro-grid Laboratory an energy self-sustaining entity with a wide range of opportunities for research, technological development and innovation. According to the conclusions reported in [24], the laboratory is a Latino-American benchmark since it is the most well-equipped in the region. Among the technical equipment available stands out three electric vehicles (a car and two vans), five urban electric bicycles, one electric mountain bicycle, and two electric mopeds that have motivated a line of research focused on electromobility, the object of this research work.

From a technical point of view, the effective implementation of the electromobility strategies mentioned entails a series of impacts on the electrical network. The most evident is the increase in the demand for electrical energy caused by the massive connection of vehicles at different points of the network to charge their batteries, which is a problem for electricity distribution companies. Particularly in the case of electric micromobility users scattered throughout the electric coverage area of a city, it is essential to characterize their short-term power consumption profile. This information enables assessing the possible effects on the energy quality presented by battery charging systems, especially when there are a lot of users. A characterization of this energy consumption will provide the distribution company with invaluable input for planning and carrying out studies of the impact on the network of residential consumers with loads intended for electromobility.

This work presents a detailed study to calculate the energy efficiency of a commercial model of an urban e-bike charged with an isolated charging station based on a photovoltaic solar source, implemented with equipment from the inventory of the electrical Microgrid Laboratory of the CCTI-B. The electric autonomy tests of this electric means of transportation are carried out through actual trips in the city of Cuenca, taking care of using the existing cycle routes in most cases.

Besides presenting the methodology used to estimate the autonomy of the electric bicycle, the paper describes a procedure leading to the characterization of the electrical profile of energy consumption during the charging hours of its battery. Also, it contains an evaluation of the affectation on the quality of energy supplied by the grid assessed under the Ecuadorian grid code ARCERNNR 002/20. The study aims to obtain a primary input to evaluate the impact that the massification of these new actors would have on the electricity distribution network and to face this new paradigm of urban mobility.

2. Materials and Methods

2.1. E-bike under study

The electric vehicle under study is an e-bike of the brand ECOMOVE, model TIV, shown in Figure 1. It belongs to the Microgrid Laboratory, a part of the CCTI-B, Universidad de Cuenca. The electrical tests performed on the e-bike, which are described below, were non-invasive. In other words, the vehicle's internal components were never accessed or tampered with.

This urban e-bike weighs 25 kg and is made of 6061 aluminum alloy. It has a 36 V/10 Ah Lithium-Ion (Li-ion) battery and a 36 V/250 W Brushless Gearless Hub Motor in the back or rear wheel. It has a maximum speed of 28 km/h and an autonomy of 30 km when driven in electric assist mode.

Figure 1. E-bike ECOMOVE model TIV under study

The battery's nominal electrical energy storage capacity does not appear in the manufacturer's datasheet. However, using the charging capacity (10 Ah) and average battery voltage (36 V_{DC}) for calculation resulted in 0.360 kWh.

The battery charger is the model KYLC084V42J – Class II, manufactured by WuXi KeYu Electronic Technology Co., Ltd., and designed for 42V lithium-ion rechargeable batteries. The device's AC input supports a nominal voltage of 100 to 240 V_{AC}, at a frequency of 50 to 60 Hz, and a maximum RMS current of 1.8 A. The DC output offers 42 V_{DC} and a maximum average current of 2 A (with protection fuse T/3.15 A/250 V, slow action).

2.2. Route planned to discharge the e-bike's battery

A 34 km route (approx.) was planned, allowing the use of the cycle routes in Cuenca. The Microgrid Laboratory, located in Campus Balzay, is the point of departure and arrival. A GPS watch is used to calculate the actual distance traveled. This device records geolocation data and other parameters of interest to the user, such as the linear speed of movement (km/h) and heart rate (bpm). Figure 2 shows the entire route, with five reference points identified.

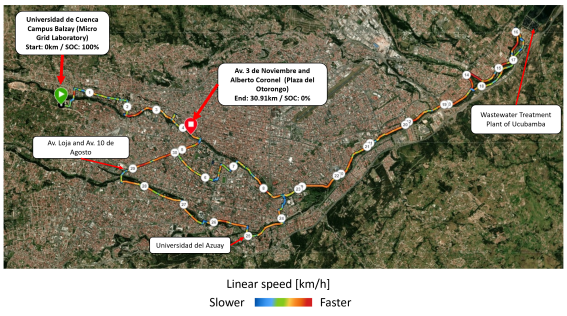

Figure 2. Route traveled with the e-bike. White bubbles with numbers identify each kilometer traveled. The geolocation data was recorded with the GPS device

The departure where the entire battery's state of charge (SOC) is available (SOC = 100%); the arrival where the battery has been fully discharged (SOC = 0%); it is no longer possible to use the electric assist mode of the e-bike; and three additional reference points so the reader can easily recognize the route traveled.

2.3. Standalone solar photovoltaic charging station

A solar photovoltaic charging station isolated from the power grid is implemented in the Microgrid Laboratory to recharge the e-bike's battery, using an Ampere Square Pro (ASP) energy storage and management system based on lithium batteries.

The ASP has five main components starting with a 6-kWh lithium-ion battery (BT). A 3-kW hybrid bidirectional inverter (INV) to carry out the DC-AC and AC-DC power conversions. An energy management system (EMS) manages the energy to regulate the charge/discharge cycles of the device. It has a bidirectional energy meter to register generation and consumption; and electrical protections (B1, B2, ..., and B5) to look after the main components and to perform command actions.

Also, five polycrystalline solar panels of 38 V at a maximum power of 335 W, series-connected, supply energy to the ASP. The panels are installed on the roof of the laboratory building, as can be seen in Figure 3.

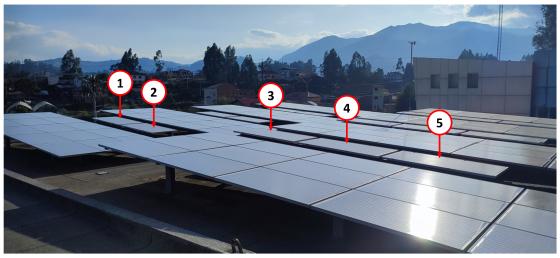

1, 2, 3, 4, and 5: polycrystalline solar panels model A-335P GS manufactured by ATERSA

Figure 3. Solar panels installed on the terrace of the Microgrid Laboratory. The five series-connected panels indicated and numbered in the picture are series-connected to the PV String 1 input of the Ampere Square Pro energy storage system

Figure 4 shows the complete standalone solar photovoltaic charging station, pointing out its main components. The photograph shows the measurement equipment installed at the outlet of the charging station.

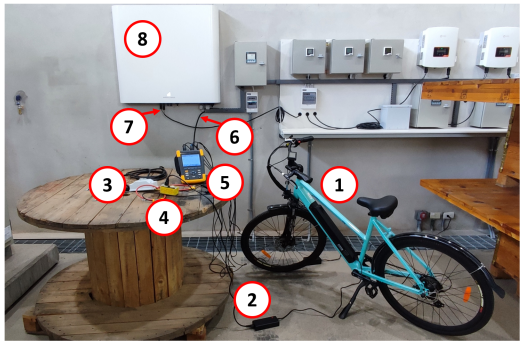

1. E-bike.
2. Battery charger.
3. Outlet at 127 VAC/60Hz.
4. Thermomagnetic protection.
5. Power Quality and Energy Analyzer Fluke 435 Series II.
6. AMPERE Square PRO's output at 127 VAC/60Hz.
7. AMPERE Square PRO's input (PV string 1), 190 V_{DC} at maximum power, 1675W, from the 5 series-connected solar panels.
8. AMPERE Square PRO.

Figure 4. Standalone solar photovoltaic charging station for e-bikes implemented in the Microgrid Laboratory. The e-bike under study is being recharged

Figure 5 shows the electrical diagram of the standalone charging station. An energy & power quality analyzer that fulfills the international standards IEC 61000-4-7, IEC 61000-4-30, and IEEE Std 519-2014 measures the energy consumption of the e-bike and records the variables of interest.

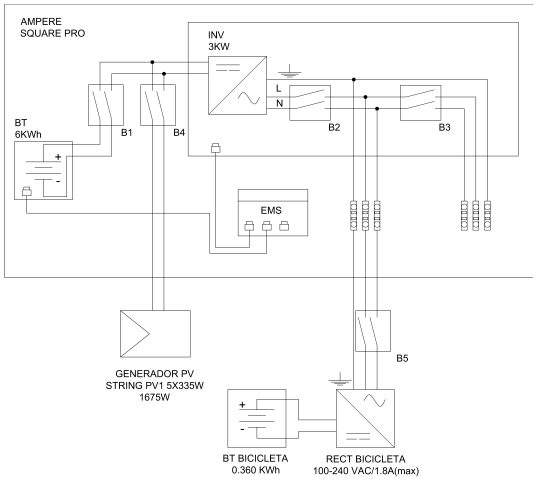

Figure 5. Electrical diagram of the standalone solar photovoltaic charging station implemented in the Microgrid Laboratory. Source: Own elaboration based on the diagrams available in [25]

The only connected load is the e-bike under study. The analyzer works in logger mode to take measurements from an AC single-phase system with line and neutral 127 V_{RMS} nominal, using two voltage terminals and two current probes (one for neutral) with a recording interval of one second. The electrical variables recorded are in line to neutral (L-N) voltage, phase current, frequency, distortion power factor, displacement power factor, current and voltage total harmonic distortion, current and voltage harmonic components (H2, H3, ..., H11), crest factor of current and voltage, flicker, active power, apparent power, and active energy consumed (Wh).

2.4. Ecuadorian grid code ARCERNNR 002/20

The Ecuadorian grid code ARCERNNR 002/20 entitled Quality of the Electricity Distribution and Commercialization Service has the purpose of: "Establishing the indicators, indices, and limits of quality of the service of distribution and commercialization of electrical energy; and defining the measurement, registration and evaluation procedures to be fulfilled by the electricity distribution companies and consumers, as appropriate" [26, p. 4].

For this research, the quality attribute of interest is at the consumer's side, stated in section 5.2 of [26] as Consumer Quality Aspect and evaluated through the current harmonic distortion. According to section 29 of [26], the indexes to evaluate the current's individual harmonic distortion and its total demand distortion (also known as the current's total harmonic distortion, THD) are calculated as follows:

$$I_{h,k} = \sqrt{\frac{1}{200} \cdot \sum_{i=0}^{200} (I_{h,i})^2} \quad (1)$$

$$DI_{h,k} = \frac{I_{h,k}}{I_{h,1}} \cdot 100\ [\%] \quad (2)$$

$$THD_k = \left[\frac{1}{I_{h,1}} \cdot \sqrt{\sum_{h=2}^{50} (I_{h,k})^2} \right] \cdot 100\ [\%] \quad (3)$$

Where: $I_{h,k}$ is the h^{th} current's harmonic in the k^{th} 10-minute range as required by the standard IEEE Std 519-2014; $I_{h,i}$ is the effective value (RMS) of the h^{th} current's harmonic (for h = 2, 3,..., 50) measured every three seconds (for i = 1, 2, 3,..., 200); $DI_{h,k}$ is the individual distortion factor of the h^{th} current's harmonic (for h = 2, 3, ..., 50) in the k^{th} 10-minute range; THD_k is the current's total harmonic distortion in the k^{th} 10-minute range; and $I_{h,1}$ is the effective value (RMS) of the fundamental component of the current (60 Hz).

Table 1 shows the maximum levels for the current's individual and total harmonic distortion, taken from section 29.2 of [26], only up to the 17th harmonic component for this study.

Table 1. Maximum levels for the current's odd harmonic components [a] as a percentage of the maximum demand current at fundamental frequency (60Hz) [26]

ICC/IL	3 ≤ h < 11	11 ≤ h < 17	TDD (THD-A)
< 20 [b]	4.0	2.0	5.0
20 < 50	7.0	3.5	8.0
50 < 100	10.0	4.5	12.0
100 < 1000	12.0	5.5	15.0
> 1000	15.0	7.0	20.0

a The limits for even harmonics are the 25% of the limits shown in this table.
b All the equipment is limited to these values of current distortion, where: I_{CC} = maximum current of short circuit at the point of common coupling (PCC): and, I_L = maximum load current at fundamental frequency (60Hz)

Section 29.4 of the grid code establishes that consumers fulfill at the measurement point the current's individual harmonic distortion factor $DI_{h,k}$ and the current's total harmonic distortion factor THD_k, both calculated using equations (1), (2), and (3) when 95% or more of the data registered during an evaluation period of at least seven days are between the limits listed in Table 1.

This research uses the indexes and limits specified by the Ecuadorian grid code [26] to analyze the impacts on the power grid of charging the e-bike by processing the data of the lithium-ion battery's charging entire regime, which takes a few hours to complete.

3. Results and discussion

One of the technicians of the Microgrid Laboratory (male, 36 years old, 73 kg of weight and 1.73 m of height) used the e-bike under study to ride through the previously planned route, only using the electric assist mode of the vehicle. All the electrical energy stored in the battery drained over 30.91 km of distance in two hours, ten minutes and thirty-five seconds (02:10:35), with an average linear speed of 14.2 km/h. So, the experiment achieved a full discharge in ordinary battery operation.

The battery charging process started in the Microgrid Laboratory, connecting the charger to the standalone solar photovoltaic charging station as its only load. It is necessary to mention that the charger stayed connected even after it turned on the light signal of fully charged to register data of the last charging stage of the battery, known as the float charge state. The following is an analysis of the data, acquired by the energy & power quality analyzer.

3.1. Energy quality analysis

The lithium-ion battery's charging process was 6.77 hours long (06:46:06), and the analyzer took 24366 measurements of the electrical variables of interest. The average measured values of the AC RMS phase to neutral voltage ($V_{F\text{-}N}$) connected to the input of the battery charger are 127.24 V at a frequency (f) of 59.95 Hz. The equipment registered an average crest factor (CF-V) of 1.42, with a maximum value of 1.43 over the entire measurement range.

Regarding the AC RMS phase current (I_F) the analysis of the average measurements registered shows that the charger performs a charging regime named IUoI specified by the German standards DIN 41772 [27], Supplement 1 to DIN 41772 [28], and DIN 41773-1 [29]. The goal of this standardized regime is to charge the battery in a relatively short time without affecting its useful life, and to keep the charge in the battery while the charger remains connected.

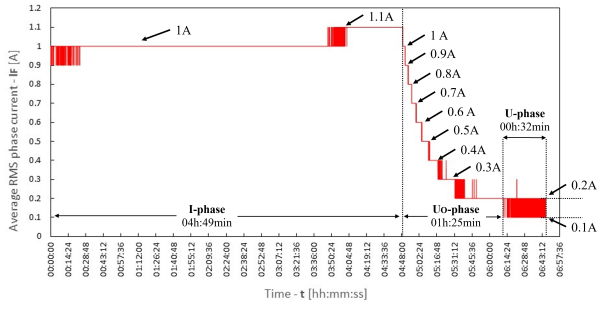

Figure 6. The average RMS phase current (I_F) data registered throughout the charging period show the three stages of the charging regime IUoI

Data shows that the charging regime carried out by the charger of the e-bike under study consists of 3 well-defined stages (refer to Figure 6). The following is a brief description of these stages.

I-phase. Also called the bulk charge stage. The charger provides a constant charging current to the battery when there is a deep discharge. The voltage increases without exceeding Umax (which can be a fixed value or dependent on temperature), and the battery absorbs the charge. When the battery terminals reach Umax, the charger goes to phase Uo.

The charger operated in the I-phase stage for 4 hours and 49 minutes; the average RMS phase current I_F applied was 1 A; the average active power delivered was 81.30 W; and the charging station supplied 385 Wh of active energy to the e-bike's charger.

Uo-phase. Known as the constant-voltage boost stage or absorption stage. Here the charger maintains a constant overvoltage at the battery terminals while the charging current decreases. This voltage value is not safe for an indefinite application, but it allows charging the battery in less time. According to [29] , the maximum voltage should be between 2.33 V and 2.40 V per cell, depending on the battery's design and operating conditions. This phase ends when the charging current reaches a minimum threshold I_{min}, and the charger passes to phase U.

In this stage, the average RMS phase current I_F applied decreases from 1.1 A to 0.2 A (I_{min}) in 1 hour and 25 minutes. Figure 6 shows that the decrease of the charging current occurs in 0.1 A steps. Throughout the Uo-phase, only 34 Wh were supplied to charge the e-bike's battery. As a result, at the end of the stage, the total active energy provided by the charging station to the charger is 419 Wh in 6 hours and 14 minutes. At this point, the battery is fully charged (SOC = 100%).

U-phase. This last stage is called the float charge stage. The charger applies a voltage safe to maintain for longer periods without significantly affecting battery's life. In this stage, the current decreases to a residual value, making it possible to compensate for the battery's self-discharge.

Since the charger remained connected even after it turned the light signal of fully charged on to register data of the U-phase stage, it was possible to determine that the residual value of the charging current is 0.1 A. Figure 6 shows that in this stage, the charging current stays at 0.1 A and commutes to 0.2 A for a few seconds to compensate the battery's self-discharge. This behavior keeps happening while the charger is connected to the station. In 32 minutes, the station supplied only 3 Wh to the charger, for the compensation.

A well-known fact about lithium-ion batteries is that they do not need charging up to 100% to prolong the battery's life by avoiding the overvoltage of the second stage of the charging regime shown in Figure 6. Because measurements prove that 91.89% of the

total electrical energy supplied by the charging station to the charger (385 Wh out of 419 Wh, see Figure 7) occurred in the I-phase, the forthcoming analysis focuses on the electrical parameters of interest registered during the I-phase.

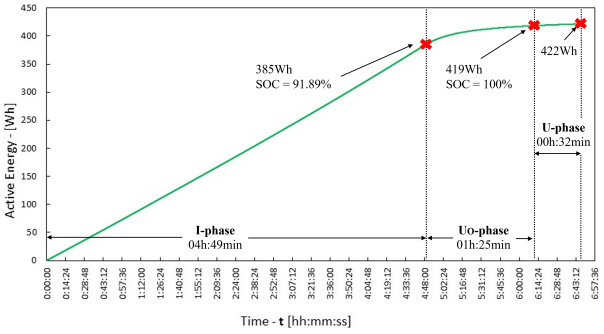

Figure 7. Active energy measured in Wh delivered to the charger during the charging process

Regarding total harmonic distortion, THD-V for the voltage $V_{F\text{-}N}$ and THD-A for the charging current I_F, the measured values were 4.71% and 106.01%, respectively. The total power factor of the charger is 0.62, calculated by multiplying the average registered values of displacement power factor (PF) and distortion power factor (DPF), 0.63 and 0.99, respectively, since the charger is a non-linear load.

The odd harmonic components of the phase current I_F are responsible for the high values of THD-A and the low total power factor, especially the components H3, H5 and H7, whose average magnitudes are 80.71%, 57.14% and 32.41% of the fundamental, respectively. Figure 8 shows the behavior of the first five odd harmonic components of I_F for the entire charging regime.

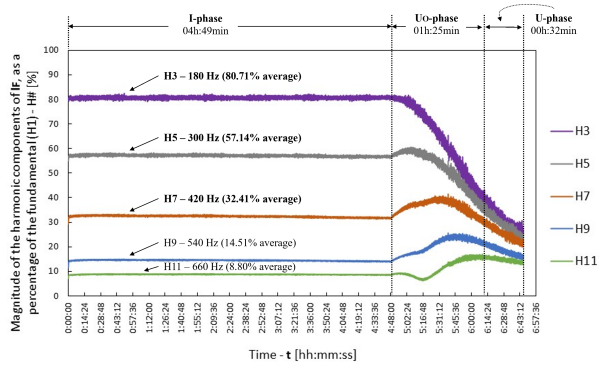

Figure 8. Measured average values of the odd harmonic components (H3, H5, H7, H9 and H11) of the charging current I_F. The measuring equipment calculates these and other data in a time window of 200 ms according to the IEC 61000-4-7 standard for FTT fast Fourier transform algorithms

At 3 hours and 51 minutes of charging during the I-phase, the waveform of the charging current I_F shown in Figure 9 results from the effect of its odd harmonic components. The high value of THD-A makes sense by only looking at the waveform. Regarding the waveform AC RMS phase to neutral voltage $V_{F\text{-}N}$, also presented in Figure 9, it is possible to notice its closeness to a perfect sinusoidal. However, the absolute instant values of $V_{F\text{-}N}$ slightly decrease when I_F goes up to its maximum positive value and negative minimum (highlighted in blue circles in figure 8), which justifies the 4.71% of the measured THD-V.

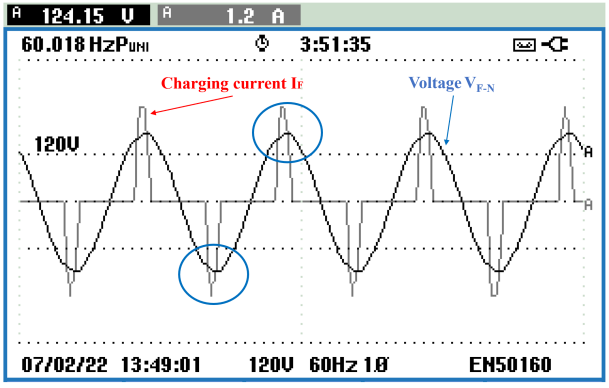

Figure 9. Waveforms of the charging current I_F and phase to neutral voltage $V_{F\text{-}N}$ taken by the oscilloscope of the energy & power quality analyzer at 3 hours and 51 minutes of charging during the I-phase

Concerning the Ecuadorian grid code ARCERNNR 002/20, the limits for the magnitude of the individual charging current's odd harmonic components as a percentage of the fundamental and its total harmonic distortion differ in different ranges of the relationship between the maximum short circuit current at the point of common coupling and the maximum load current of fundamental frequency (H1), named I_{CC}/I_L (refer to Table 1). The grid code mandates that the magnitude of the first four odd harmonics cannot exceed 15% in all the ranges. Likewise, the current's total harmonic distortion (THD-A) should never exceed 20%.

In this context, the measurements of the parameters above-mentioned (H3 = 80.71%, H5 = 57.14%, H7 = 32.41%, H9 = 14.51%, and THD-A = 106.01%) exceed the limits established by the grid code regarding the consumer quality aspect, which has to be accounted to evaluate the impact of a future large-scale utilization of e-bikes (brand and model under study, and others) in Ecuador.

3.2. Energy efficiency analysis

According to [30], the user's habits determine an e-bike's energy efficiency. It also mentions that no unique metric exists to study this critical parameter. However, it suggests that manufacturers often use the number of kWh per 100 miles to inform their products' energy

efficiency ranges. Thus, the charger's 419 Wh (0.419 kWh) absorbed in 6 hours and 14 minutes at the end of the Uo-phase is the battery's actual electrical energy storage capacity (SOC = 100%), assuming the losses in the charger are neglectable. Since this amount of electrical energy drained over the 30.91 km ride (19.21 miles) during the experiment, then the average energy efficiency of the e-bike under study is:

$$\eta_{E(kWh-100miles)} = \frac{E}{d} \cdot 100 \tag{4}$$

Where η_E is the average energy efficiency measured in kWh/100miles, d is the distance in miles, and E is the battery's electrical energy stored at SOC = 100% in kWh. The result of substituting terms in (4) is 2.18 kWh/100miles. With the Ecuadorian national average rate of 0.092 USD per kWh, the cost of riding 100 miles with the e-bike under study is 0.2 USD (20 cents).

The number of meters the e-bike can go per watt-hour of electrical energy stored in its battery is also helpful in evaluating energy efficiency, which is calculated as follows:

$$\eta_{E(m/Wh)} = \frac{E}{d} \tag{5}$$

With $d = 30910$ m and $E = 419$ Wh, the calculation results in 73.77 m/Wh for the vehicle under study.

The USA's Environmental Protection Agency (EPA) defines the term miles per gallon equivalent or MPGe to rate the efficiency or fuel economy of electric vehicles (EVs). It compares the amount of electric energy required to charge EVs to the energy provided by a gallon of gas. According to EPA estimations, the energy provided by one gallon of gas is 33.7 kWh. So, the 0.419 kWh required to charge the e-bike entirely is equivalent to 0.0124 gallons of gas. Since the e-bike covered 19.21 miles with that amount of energy, its MPGe is calculated as follows:

$$MPGe = \frac{d}{G} \tag{6}$$

Where d is the distance covered by the e-bike measured in miles, and G is the gallons of gas equivalent previously calculated. The substitution of terms results in 1545.1 MPGe, which is 12 times fold the fuel economy of a 2022 Tesla Model 3 RWD (132 MPGe), the highest-ranked EV in the Fuel Economy Guide Model Year 2022 of the US Department of Energy [31]. The last statement exemplifies the potential benefits of micromobility vehicle usage.

4. Conclusions

The research carried out in the Microgrid Laboratory of Universidad de Cuenca analyzes the energy behavior of an urban e-bike of the brand ECOMOVE, model TIV, on a route of 30.91 km in the urban area of Cuenca, in electric assistance mode only. A solar photovoltaic charging station isolated from the power grid was implemented in the laboratory. The station has five polycrystalline solar panels of 335 W each, series-connected; an energy storage and management system; and electrical protections. To estimate the energy consumption of the e-bike and record the variables of interest, a power quality and energy analyzer was used.

The average AC RMS phase current data analysis shows that the e-bike's battery charger applies an IUoI charging regime standardized by the German regulations DIN41772, Supplement 1 to DIN 41772, and DIN 41773-1, with three well-defined stages. First, the bulk charge stage (I-phase), in which the charger receives a constant current of 1 A for about 4.82 hours, delivers 91.89% of the charge to the battery, and raises the voltage at its terminals. Then, the constant-voltage boost stage (Uo-phase), where the charging current decreases in discrete steps of 0.1 A, from 1.1 A to a minimum value of 0.2 A in about 1.42 hours, and only delivers the 8.11% of charge remaining. Finally, the charger reaches the float charge stage (U-phase) to solely compensate battery's self-discharge by applying 0.2 A for short periods, when required. At this point, the reader has a characteristic model of the load profile of a micromobility transport, which will allow carrying out electrical network studies related to massifying this type of consumer.

Moreover, measurements show that the battery's actual electrical energy storage capacity is 419 Wh, approximately. This capacity provides an autonomy of 30.91 km, measured through a previously planned urban route and only using the electric assist mode of the vehicle. Therefore, the estimated average energy efficiency of the e-bike under study is 2.18 kWh/100miles or 73.77 m/Wh, and a fuel economy of 1545.1 MPGe. Hence, the cost of riding 100 miles is 0.2 USD (20 cents).

About 92% of the total electrical energy supplied by the charging station to the charger, 385 Wh out of 419Wh, occurred in the first stage of the charging regime (I-phase). The charging current is constant and presents its highest average value, 1 A. Hence, the I-phase data are the most relevant for energy quality analysis.

Data analysis proves that the total power factor of the charger is 0.62, and the total harmonic distortion of the charging current (THD-A) is 106.01%, primarily due to its first three odd harmonic components, H3, H5, and H7, whose average magnitudes are 80.71%, 57.14% and 32.41% of the fundamental, respectively. The voltage waveform is close to a perfect sinusoidal, which is proven by a total harmonic distortion (THD-V) of 4.71%.

According to the technical specifications for assessing the consumer quality aspect of the Ecuadorian grid code ARCERNNR 002/20, the magnitudes of the individual charging current's odd harmonic components as a percentage of the fundamental (H3 = 80.71%, H5 = 57.14%, H7 = 32.41%, and H9 = 14.51%, and the charging current's total harmonic distortion (THD-A= 106.01%) are well above the limits established by the grid code. For a future large-scale use of e-bikes as a means of transportation in the urban centers of Ecuador, the vehicles' charger's fulfillment of the law in force must be checked beforehand.

Acknowledgments

The work documented in this manuscript is part of the activities carried out in the project entitled: "Movilidad Eléctrica: retos, limitaciones y plan de implementación en el régimen especial de la Provincia de Galápagos enfocada en el desarrollo sostenible y su factibilidad en la Ciudad de Cuenca", II Concurso de Proyectos de Investigación – Vinculación, Vicerrectorado de Investigación y la Dirección de Vinculación con la Sociedad de la Universidad de Cuenca. The authors thank Universidad de Cuenca for easing access to the facilities of the Microgrid Laboratory of the Centro Científico Tecnológico y de Investigación Balzay (CCTI-B), for allowing the use of its equipment, and for authorizing its staff the provision of technical support necessary to carry out the experiments described in this article.

References

[1] A. Bull, *Congestión de tránsito: el problema y cómo enfrentarlo.* Comisión Económica para América Latina y el Caribe (CEPAL), Naciones Unidas, 2003. [Online]. Available: https://bit.ly/3TW587t

[2] I. Thomson and A. Bull, *La congestión del tránsito urbano: causas y consecuencias económicas y sociales.* Comisión Económica para América Latina y el Caribe (CEPAL), División de Recursos Naturales e Infraestructura, Unidad de Transporte, Naciones Unidas, 2001. [Online]. Available: https://bit.ly/3TW587t

[3] P. Felipe-Falgas, C. Madrid-Lopez, and O. Marquet, "Assessing environmental performance of micromobility using lca and self-reported modal change: The case of shared e-bikes, e-scooters, and e-mopeds in barcelona," *Sustainability*, vol. 14, no. 7, p. 4139, 2022. [Online]. Available: https://doi.org/10.3390/SU14074139

[4] M. Elhenawy, H. A. Rakha, Y. Bichiou, M. Masoud, S. Glaser, J. Pinnow, and A. Stohy, "A feasible solution for rebalancing large-scale bike sharing systems," *Sustainability*, vol. 13, no. 23, p. 13433, 2021. [Online]. Available: https://doi.org/10.3390/su132313433

[5] IEA, *Global EV Outlook 2020.* IEA. Paris, 2020. [Online]. Available: https://bit.ly/3gne4EW

[6] M. M. Sokolowski, "Laws and policies on electric scooters in the european union: A ride to the micromobility directive?" *European Energy and Environmental Law Review*, vol. 29, pp. 127–140, 2020, place: Alphen aan den Rijn, The Netherlands Publisher: Kluwer Law International. [Online]. Available: https://doi.org/10.54648/EELR2020036

[7] K. Turoń and P. Czech, "The concept of rules and recommendations for riding shared and private e-scooters in the road network in the light of global problems," in *Modern Traffic Engineering in the System Approach to the Development of Traffic Networks*, E. Macioszek and G. Sierpiński, Eds. Springer International Publishing, 2020, pp. 275–284. [Online]. Available: https://doi.org/10.1007/978-3-030-34069-8_21

[8] A. Li, P. Zhao, X. Liu, A. Mansourian, K. W. Axhausen, and X. Qu, "Comprehensive comparison of e-scooter sharing mobility: Evidence from 30 european cities," *2022*, vol. 105, p. 103229, Transportation Research Part D: Transport and Environment. [Online]. Available: https://doi.org/10.1016/j.trd.2022.103229

[9] K. Wang, X. Qian, D. T. Fitch, Y. Lee, J. Malik, and G. Circella, "What travel modes do shared e-scooters displace? a review of recent research findings," *Transport Reviews*, pp. 1–27, 2022. [Online]. Available: https://doi.org/10.1080/01441647.2021.2015639

[10] E. Ayyildiz, "A novel pythagorean fuzzy multi-criteria decision-making methodology for e-scooter charging station location-selection," *Transportation Research Part D: Transport and Environment*, vol. 111, p. 103459, 2022. [Online]. Available: https://doi.org/10.1016/j.trd.2022.103459

[11] M.-D. Lin, P.-Y. Liu, J.-H. Kuo, and Y.-H. Lin, "A multiobjective stochastic location-allocation model for scooter battery swapping stations," *Sustainable Energy Technologies and Assessments*, vol. 52, p. 102079, 2022. [Online]. Available: https://doi.org/10.1016/j.seta.2022.102079

[12] Y.-W. Chen, C.-Y. Cheng, S.-F. Li, and C.-H. Yu, "Location optimization for multiple types of charging stations for electric scooters," *Applied Soft Computing*,

vol. 67, pp. 519–528, 2018. [Online]. Available: https://doi.org/10.1016/j.asoc.2018.02.038

[13] J. G. Schmidt, F. J. De Faveri, J. C. De Bona, E. A. Rosa, L. S. Dos Santos, C. Q. Pica, L. B. R. Morinico, and I. França, "Forecasts and impact on the electrical grid with the expansion of electric vehicles in northeast of brazil," in *2022 IEEE/PES Transmission and Distribution Conference and Exposition (T&D)*, 2022, pp. 1–5. [Online]. Available: https://doi.org/10.1109/TD43745.2022.9816978

[14] L. Di Chiara, F. Ferres, and F. Bastarrica, "Impact of electromobility deployment scenarios in the power system of uruguay by 2028," in *2021 IEEE URUCON*, 2021, pp. 360–363. [Online]. Available: https://doi.org/10.1109/URUCON53396.2021.9647426

[15] D. P. Jaramillo, M. C. Gutiérrez, and R. Mix, *Electromovilidad: Panorama actual en América Latina y el Caribe: Versión infográfica.* Banco Interamericano de Desarrollo, 2019. [Online]. Available: http://dx.doi.org/10.18235/0001654

[16] Primicias. (2020) Las ventas de vehículos híbridos y eléctricos crecen casi 300 %. [Online]. Available: https://bit.ly/3EM9mZR

[17] J. Figura and T. Gadek-Hawlena, "The Impact of the COVID-19 Pandemic on the Development of Electromobility in Poland. The Perspective of Companies in the Transport-Shipping-Logistics Sector: A Case Study," *Energies*, vol. 15, no. 4, pp. 1–18, 2022. [Online]. Available: https://bit.ly/3XkWfaj

[18] T. Rokicki, P. Bórawski, A. Beldycka-Bórawska, A. Zak, and G. Koszela, "Development of electromobility in european union countries under covid-19 conditions," *Energies*, vol. 15, no. 1, 2022. [Online]. Available: https://doi.org/10.3390/en15010009

[19] GAD Cuenca. (2022) Plan de movilidad. [Online]. Available: https://bit.ly/3EPQlqh

[20] P. Ochoa, *Ciclovía de los Ríos de Cuenca.* GAD Municipal de Cuenca, 2018. [Online]. Available: https://bit.ly/3ETFQCw

[21] C. A. Cruz Leal and M. Virviescas Arias, "Evaluación de la operación del tranvía de cuenca ecuador y del tranvía de medellín colombia," 2018.

[22] Redacción El Mercurio. (2021) Nueva electrolinera en Cuenca. [Online]. Available: https://bit.ly/3vnx7CY

[23] J. L. Espinoza, L. G. González, and R. Sempértegui, "Micro grid laboratory as a tool for research on non-conventional energy sources in ecuador," in *2017 IEEE International Autumn Meeting on Power, Electronics and Computing (ROPEC)*, 2017, pp. 1–7. [Online]. Available: https://doi.org/10.1109/ROPEC.2017.8261615

[24] J. M. Rey, G. A. Vera, P. Acevedo-Rueda, J. Solano, M. A. Mantilla, J. Llanos, and D. Sáez, "A review of microgrids in latin america: Laboratories and test systems," *IEEE Latin America Transactions*, vol. 20, no. 6, pp. 1000–1011, 2022. [Online]. Available: https://doi.org/10.1109/TLA.2022.9757743

[25] AMPERE ENERGY, *AMPERE square PRO Manual del instalador.* AMPERE POWER ENERGY S.L., 2021. [Online]. Available: https://bit.ly/3ABgxm4

[26] ARCERNNR, *Calidad del servicio de distribución y comercialización de energía eléctrica.* Agencia de Regulación y Control de Energía y Recursos Naturales no Renovables, 2020. [Online]. Available: https://bit.ly/3tRydGr

[27] DIN, *DIN 41772 Static power convertors; semiconductor rectifier equipment, shapes and letter symbols of characteristic curves.* German Institute for Standardisation (Deutsches Institut für Normung), 1979. [Online]. Available: https://bit.ly/3GCFD8b

[28] ——, *DIN 41772 Supplement 1 Static power convertors; semiconductor rectifier equipment, examples of characteristic curves for battery chargers.* German Institute for Standardisation (Deutsches Institut für Normung). [Online]. Available: https://bit.ly/3GCJTEp

[29] ——, *DIN 41773-1 Static power convertors; semiconductor rectifier equipment with IU-characteristics for charging of lead-acid batteries, guidelines.* German Institute for Standardisation (Deutsches Institut für Normung). [Online]. Available: https://bit.ly/3hSi28X

[30] T. McCarran and N. Carpenter, "Electric bikes: Survey and energy efficiency analysis," *Efficiency Vermont*, 2018. [Online]. Available: https://bit.ly/3ACmgYP

[31] Department of Energy. (2022) Fueleconomy.gov Top Ten. [Online]. Available: https://bit.ly/3VdjKjy